JOURNAL OF APPLIED ELECTROCHEMISTRY 23 (1993) 927–932

Experimental investigation of the terminal effect in lead electrodeposition onto resistive substrates

P.-H. VALLOTTON, M. MATLOSZ, D. LANDOLT

Laboratoire de Métallurgie Chimique, Département des Matériaux, Ecole Polytechnique Fédérale de Lausanne, MX-C Ecublens, CH-1015 Lausanne, Switzerland

Received 29 September 1992; revised 26 November 1992

The nonuniformity of the current distribution during electroplating onto resistive electrodes is investigated experimentally for the deposition of lead onto thin nickel–phosphorous substrates. Profiles of deposit thickness along the substrate surface are obtained and the kinetic parameters needed for modeling are evaluated. The experimental data are compared to numerical simulations, and limitations of the theoretical treatment are discussed.

List of symbols

a	substrate thickness (cm)
b	electrodeposit thickness (cm)
b_{avg}	average electrodeposit thickness (cm)
B	dimensionless electrodeposit thickness
c_b	bulk concentration (mol cm^{-3})
c_n	Fourier series coefficient
d	distance between counterelectrode and cathode (cm)
D	dimensionless counterelectrode distance
D	diffusion coefficient (cm^2 s^{-1})
E	dimensionless overpotential
E_{rev}	reversible electrode potential (V)
F	Faraday constant (96 487 C mol^{-1})
i	current density (A cm^{-2})
i_{avg}	average current density (A cm^{-2})
i_c	local current density along the cathode (A cm^{-2})
i_0	exchange current density (A cm^{-2})
I	dimensionless current density
K	dimensionless average cathode resistance
K_0	dimensionless initial cathode resistance
L	cathode length (cm)
n	Fourier series index
R	ideal gas constant (8.314 J mol^{-1} K^{-1})
R_Ω	ohmic resistance (Ω cm^2)
s	cathode conductance (Ω^{-1})
t	time (s)
T	absolute temperature (K)
V	potential (V)
Wa_L	Wagner number for linear kinetics
Wa_T	Wagner number for Tafel kinetics
x	distance along the cathode from current collector corner (cm)
X	dimensionless distance
z	valence

Greek symbols

α	symmetry coefficient
β_a	anodic Tafel constant (V)
β_c	cathodic Tafel constant (V)
η	overpotential (V)
κ	electrolyte conductivity (Ω^{-1} cm^{-1})
ρ	molar density of the electrodeposit (mol cm^{-3})
σ_a	substrate conductivity (Ω^{-1} cm^{-1})
σ_b	deposit conductivity (Ω^{-1} cm^{-1})
τ	dimensionless deposition time (=dimensionless average deposit thickness)
ω	angular disk rotation speed (rad s^{-1})
ν	kinematic viscosity (cm^2 s^{-1})

1. Introduction

Electrochemical deposition of metals and alloys is commonly employed in the electronics industry for the fabrication of thin films on printed circuits. When films are deposited onto substrates such as electroless seed layers that present a high ohmic resistance, the electrodeposition reaction tends to concentrate near the current collector. This phenomenon, often referred to as the terminal effect, leads to nonuniform deposit thickness, and sometimes to nonuniform alloy composition.

A number of authors have investigated the terminal effect for a variety of applications and cell geometries, and a comprehensive list of references on the subject has been given in a previous paper [1]. Most of these studies have been theoretical in nature and only a few have presented experimental results. Fomichev [2] studied the distribution of the current density for oxygen evolution on a plate strip platinum anode in $HClO_4$ solution, while Conway *et al.* [3] studied oxygen evolution on a long, thin platinum wire immersed in H_2SO_4 solutions. D'Amico *et al.* [4] tested the theoretical treatment of Tobias and Wijsman [5] for the deposition of copper onto thin moving strips. More recently Bisang and Kreysa [6, 7] tested their own theoretical models by measuring the current distribution on a platinum wire for oxygen evolution in H_2SO_4 and for hydrogen generation in NaOH solutions. Most authors found good agreement between the experimental results and their theo-

0021-891X

retical predictions, but the models used in these studies are restricted to a number of particular cases and, with the exception of D'Amico *et al.*, none address the electrodeposition of metallic films.

In the plating of thin metallic films onto resistive substrates the current distribution depends on several interacting phenomena, including the substrate resistance, surface and concentration overpotentials, electrolyte resistance, counterelectrode position, deposition kinetics, and growth of the depositing layer. In a recent paper [1], a general theoretical analysis of this problem was developed by extending the analytical treatment of Tobias and Wijsman [5] to include nonlinear effects such as Tafel polarization and varying substrate conductance due to the growth of the depositing film. Comparison of approximate solutions to exact numerical results from the general model was used to establish a list of criteria, based on the values of a few characteristic dimensionless groups, for the selection of appropriate simplified models in specific cases.

The purpose of the present paper is to evaluate experimentally the terminal effect in a realistic electrodeposition system, and subsequently to compare the experimental results to the theoretical predictions of the previous work. The electrodeposition of a thin film of lead onto a resistive, electroless nickel–phosphorous substrate is used as a model experimental system. Electrodeposition of lead–tin alloys is used in the fabrication of thin layers of solder for the packaging of electronic devices such as quartz oscillators.

2. Polarization characteristics for Pb deposition

2.1. Experimental procedure

The kinetic parameters needed for quantitative modeling of lead electrodeposition are studied by measuring galvanostatically the cathodic polarization curve on a rotating hemisphere electrode (RHSE). Because of the possible presence of fluorides in the electrolyte (which may attack glass), all cell components except the electrodes themselves are made of polymethylmethacrylate polymer (PMMA). The cathode, designed in this laboratory [8], is a 1 cm diameter nickel capsule mounted onto a rotating cylindrical support and precoated at a current density of $50\,mA\,cm^{-2}$ with a $2\,\mu m$ layer of Pb. The capsule can be dismounted following an experiment to allow gravimetric measurements. The anode is a 35 mm diameter disc of pure lead placed 4 cm below the cathode pole. A Hg/Hg_2SO_4 reference electrode in saturated K_2SO_4 (Metrohm) is used to measure the working electrode potential. To avoid precipitation of $PbSO_4$ at the K_2SO_4 junction in the electrolye bath, the reference electrode is placed in a separate vessel connected to a Luggin capillary tip by an electrolyte bridge. The electrolyte is a typical lead fluoborate plating bath, without organic additives, containing 0.52 M $Pb(BF_4)_2$ (Riedel de Haen), 1.61 M ($100\,ml\,dm^{-3}$) HBF_4 (Riedel de Haen) and 0.24 M ($15\,g\,dm^{-3}$) H_3BO_3 (Merck). All experiments are performed at a temperature of 25 °C regulated by means of a thermostated water circulation system around the cell. The electrical conductivity of the bath κ is $0.212\,\Omega^{-1}\,cm^{-1}$.

For each measurement, the capsule is first weighed, then mounted onto the rotating system and polarized galvanostatically with an Amel 549 potentiostat at a predetermined current density until a $10\,\mu m$ thick predeposit is formed. Galvanostatic deposition experiments are then performed and the steady-state potential (established within a few seconds) is recorded. Depending on the current density, deposition times range from 18 min (at $10\,mA\,cm^{-2}$) to 18 s (at $600\,mA\,cm^{-2}$). The rotation speed is 800 r.p.m. for all experiments. Following deposition the capsule is detached, rinsed, dried and weighed again, and the surface observed with a scanning electron microscope (SEM).

2.2. Results

Electron micrographs reveal the presence of distinct grains in the lead (Pb) electrodeposits with a diameter ranging from 5 to $15\,\mu m$. The sharpness of the grains is responsible for a rough surface appearance, and although the size of the grains does not depend on the current density, grains grown at higher current densities appear sharper and more distinct from each other.

The current efficiency, calculated by comparing the measured weight of the deposit with the faradaic mass equivalent to the total charge passed, has an average value of $98.1 \pm 1.5\%$. No dependence of the current efficiency on current density was observed.

Figure 1 presents a semi-logarithmic plot of the measured polarization curve, corrected for the ohmic potential drop in the electrolyte between the cathode surface and the Luggin capillary tip ($R_\Omega = 1.125\,\Omega\,cm^2$). Similarly to previous studies of lead deposition from fluoborate electrolytes [9, 10], the results of this work indicate rapid charge-transfer kinetics. In the absence of mass-transfer limitations, the curve may be approximated by an expression of the Butler–Volmer type as follows:

$$i = i_0(\exp(\eta/\beta_a) - \exp(-\eta/\beta_c)) \qquad (1)$$

where $\eta = V - E_{rev}$, $\beta_a = RT/2\alpha F$ and $\beta_c = RT/2(1-\alpha)F$.

The transfer coefficient α can be determined from the slope of the semilogarithmic polarization curve in the Tafel region ($-\eta > 40\,mV$) where the contribution of the anodic term in Equation 1 can be neglected:

$$i = -i_0 \exp(-\eta/\beta_c) \qquad (2)$$

A fit to the curve in this region yields $\alpha = 0.62$, hence $\beta_a = 20.7\,mV$ and $\beta_c = 33.8\,mV$. The intercept at $\eta = 0$ corresponds to an exchange current density $i_0 = 35\,mA\,cm^{-2}$.

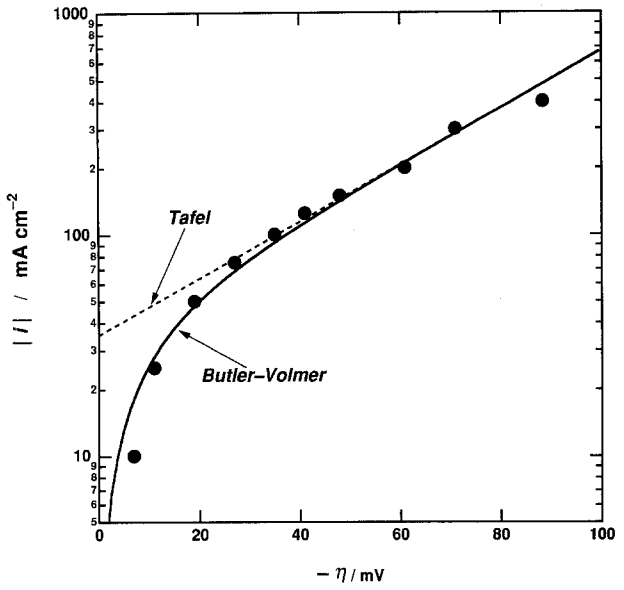

Fig. 1. Semilogarithmic plot of the ohmically corrected polarization curve for lead electrodeposition onto a rotating hemisphere electrode. (●) Experimental data; (—) Butlter–Volmer approximation of the polarization curve for $\beta_a = 20.7\,mV$; $\beta_c = 33.8\,mV$, $i_0 = 35\,mA\,cm^{-2}$; (– – –) Tafel approximation.

The polarization measurements do not indicate any mass transfer effects prior to $600\,mA\,cm^{-2}$, despite the fact that such a current density is of the same order as the theoretical limiting current density ($347\,mA\,cm^{-2}$) estimated for a smooth rotating hemispherical electrode [11] (with $\nu = 1.2 \times 10^{-2}\,cm^2\,s^{-1}$ [12], $D = 7.46 \times 10^{-6}\,cm^2\,s^{-1}$ [12], $z = 2$, $c_b = 5.2 \times 10^{-4}\,mol\,cm^{-3}$ and $\omega = 83.78\,rad\,s^{-1}$ (800 r.p.m.)). The limiting current density calculated for a smooth surface appears therefore to underestimate the actual value by about a factor of two in this case, a result which can be attributed to the additional surface provided by the roughness of the electrodeposit. Further support for this conclusion comes from the fact that the current efficiency at $600\,mA\,cm^{-2}$ is 97.4%, a value only very slightly below the average for all the experimental points (98.1%). This indicates that hydrogen evolution is not taking place and therefore that the limiting current has not yet been reached. As a result, diffusion-controlled effects should not seriously affect the global kinetics in the range chosen for the determination of the Tafel constants.

3. Lead deposition onto nickel–phosphorous substrates

Plating of lead deposits onto the resistive plates is performed in a rectangular cell with a geometry identical to the one chosen for the theoretical model [1]. The design of the experimental cell is shown in Fig. 2. Its inner dimensions are 235 mm × 50 mm × 80 mm. In order to avoid edge effects in the current distribution, the plate-shaped vertical cathode and anode are inserted in 5 mm deep troughs notched on the inside cell walls and a detachable insulating cover is fixed on the top of the cathode. With this experimental arrangement, the effective length of the cathode L is 75 mm and its width 50 mm. In all the experiments presented here, the cathode–anode distance d is 80 mm. Again, all the cell components are made of PMMA because of the possible presence of fluorides in the bath.

Stirring of the solution is accomplished by vertical vibration of a disc perforated with conical holes and attached to a cylindrical rod, as described in [13]. The vibration is performed by an electromechanical vibrator (Vibro Mixer E1, Chemap AG, Switzerland) at a frequency of 50 Hz and an amplitude of 1 mm. An empirical study of the mass-transport characteristics of this system has shown a linear relationship between the concentration of lead ions and the limiting current density [13].

The design of the resistive cathode is shown in Fig. 3. The substrate consists of a 1 μm thick electroless Ni–P layer coated onto a glass plate support. The Cr and Pd PVD flashes predeposited on the glass served as catalysts for the electroless deposition of the Ni–P layer. Conductivity measurements on a large sampling of the cathodes (by the four point method) give a mean value $\sigma_a = 1.3 \times 10^4\,\Omega^{-1}\,cm^{-1}$ (±10%), which is about 12 times smaller than the value for bulk nickel. The counterelectrode facing the cathode is a vertical plate of pure lead (99.99%).

The composition of the electrolyte is the same as

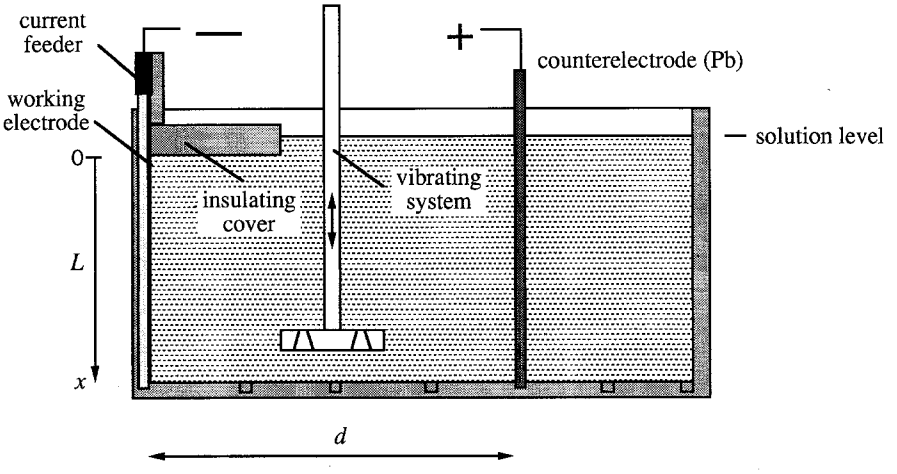

Figure 2. Schematic representation of the experimental cell for electrodeposition of lead onto resistive plate cathodes.

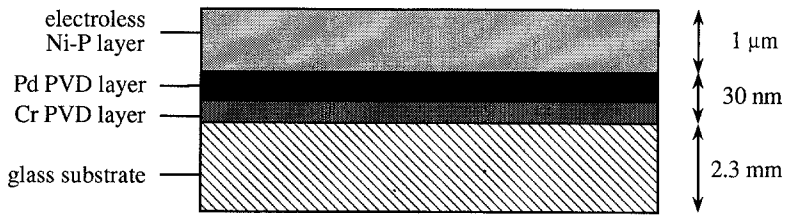

Fig. 3. Schematic cross-sectional representation (not to scale) of the resistive nickel–phosphorous cathode.

in the polarization experiments. Since both lead deposition and dissolution have nearly 100% current efficiency, the consumption of Pb^{2+} cations at the cathode is balanced by the anode dissolution, and the electrolyte concentration remains constant. At a Pb^{2+} concentration of 0.52 M, the measured average limiting current density on the cathode in the vibrated electrolyte is 230 mA cm^{-2} [13].

Prior to deposition, the substrate surface is activated by cathodic polarization in a Woods' bath (200 g dm^{-3} $NiCl_2 \cdot 6H_2O$, 75 ml dm^{-3} concentrated HCl, Pt counterelectrode) at 20 mA cm^{-2} for 2 min. Due to the low current efficiency of the bath (less than 10%) the quantity of nickel deposited in this step is less than 0.1 μm and its contribution to the substrate conductance is negligible. Hydrogen evolved on the surface during this prepolarization step assures a thorough cleaning and activation of the cathode. Deposits onto plates without pretreatment are often irregular and do not cover the whole cathode surface. Lead deposits on the Ni–P substrates are produced by electrodeposition at constant current, with the cathode connected to the circuit through a copper strip in contact with the substrate surface over its total width at the upper end of the plate. Two average applied current densities (20 and 60 mA cm^{-2}) and three deposit thicknesses (2, 5 and 10 μm) are investigated. A constant current is supplied by an Amel 555 potentiostat/galvanostat. For comparison, a series of experiments with nonresistive, 0.5 mm thick pure nickel plates are also performed under the same polarization conditions.

The thickness of the lead electrodeposits is determined by an X-ray fluorescence analyser (Fischerscope X-ray 1500, Helmut Fischer AG, Switzerland). An automatic scanning program controls the measurement of the local thickness at points regularly distributed on the cathode surface. Each point is a rectangle of 100 μm × 200 μm corresponding to the cross-sectional area of the X-ray beam. Since SEM photographs of the deposit surface show a grain size between 5 and 10 μm, effects of surface roughness on the measurements are unlikely. A thickness profile curve contains 10 values corresponding to regularly spaced coordinates along the vertical axis. The value for each coordinate is an average of three spots regularly spaced in the lateral (horizontal) direction. The standard deviation on these triplets is always found to be less than 4%.

Thickness profiles measured by X-ray fluorescence are shown in Fig. 4. The terminal effect appears on the resistive cathodes, on which the local thickness increases noticeably towards the current collector corner located at $x = 0$. No significant similar effect can be seen on the bulk nickel plates, although a slight but systematic decrease of the thickness with x can be observed. The decrease is independent of deposit thickness, but is greater at higher current densities, suggesting the existence of a variation in the diffusion-layer thickness along the length of the electrode. Although the convective recirculation pattern provided by the vibrating stirrer is not known the presence of a poorly mixed region near the bottom corner of the cell is possible and could explain this behaviour.

4. Discussion

Based on the theoretical analysis developed in the previous paper [1], a model of the current and thickness distribution in the experimental system is presented below. Following the notation of [1], the expression for Butler–Volmer kinetics (Equation 2) can be cast in dimensionless form as follows

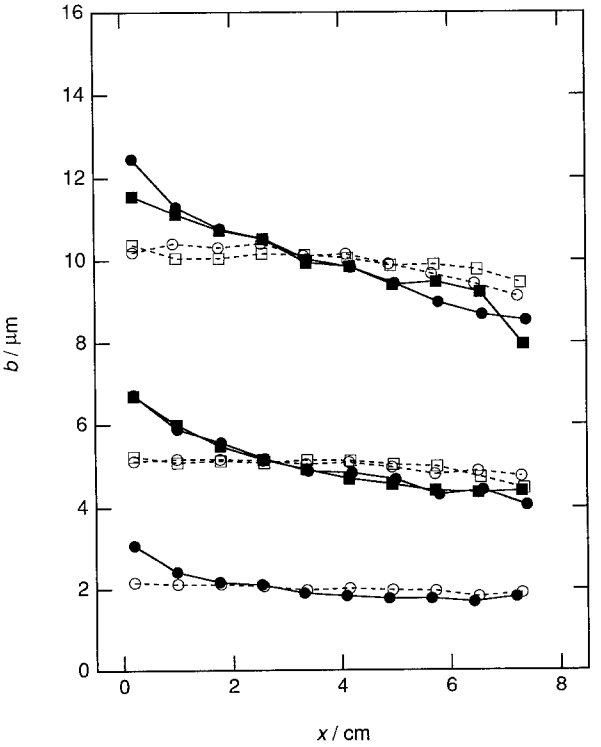

Fig. 4. Experimental thickness profiles of lead deposits on resistive nickel–phosphorous (closed symbols) and bulk nickel cathodes (open symbols). Thicknesses measured by X-ray fluorescence (● and ○) 60 mA cm^{-2}; (■ and □) 20 mA cm^{-2}.

(for cathodic deposition, $i_{avg} < 0$):

$$I = \frac{Wa_T}{Wa_L(1+\beta_c/\beta_a)}\left(\exp\left(\frac{KE}{Wa_T}\right) - \exp\left(-\frac{KE\beta_c}{Wa_T\beta_a}\right)\right) \quad (3)$$

where

$$I = i_c/i_{avg} \quad (4)$$

and

$$E = \frac{a\sigma_a + b_{avg}\sigma_b}{L^2 i_{avg}}\eta \quad (5)$$

The dimensionless current distribution $I(x/L)$ depends on five groups, that have the following values in the present experimental system (for Pb, σ_b: $= 4.85 \times 10^4\,\Omega^{-1}\,cm^{-1}$, $\rho = 0.055\,mol\,cm^{-3}$):

$$K_0 = \frac{\kappa L}{a\sigma_a} = 1.22 \quad (6)$$

$$D = d/L = 1.07 \quad (7)$$

$$Wa_T = \frac{\kappa\beta_c}{|i_{avg}|L} = 0.05 \quad (\text{for } 20\,mA\,cm^{-2}) \quad (8a)$$

$$= 0.02 \quad (\text{for } 60\,mA\,cm^{-2}) \quad (8b)$$

$$Wa_L = \frac{\kappa\beta_a\beta_c}{i_0 L(\beta_a+\beta_c)} = 0.01 \quad (9)$$

$$\beta_a/\beta_c = 0.6 \quad (10)$$

With these values, a certain number of simplifying approximations can be made based on the analysis developed in the previous paper. First, for $D = 1.07$ ($\gg 0.5$), the counterelectrode in the experimental cell (Fig. 2) is too far from the cathode to affect the path of the current lines near the surface. As a result, its actual position is unimportant and for calculation purposes it can be taken to be situated at an infinite distance ($D = \infty$) without error.

Second, since both Wa_T and Wa_L are small at the current densities studied, kinetic resistances should be negligible and the current distribution practically primary ($Wa = 0$). Under such conditions, both Wagner numbers can be taken to be zero, and the ratio β_a/β_c has no influence.

With the approximations cited above, the current density distribution and the deposit thickness should depend only on the parameter K_0. Numerical calculations performed in [1] show that for $K_0 < 5$, which is the case here, the assumption that the effect of the nonuniformity of the deposit thickness on the current distribution is negligible provides a reasonably accurate description of the behaviour. The evolution of the current density and the deposit thickness can then be estimated simply by repeated application of the Fourier cosine series:

$$I = 1 + 2\sum_{n=1}^{\infty} c_n \cos(n\pi X) \quad (11)$$

where the Fourier coefficients are defined as follows:

$$c_n = \frac{K}{K + n\pi} \quad (12)$$

and

$$X = x/L \quad (13)$$

At a given time step, K is related to K_0 as follows:

$$K = \frac{K_0}{1+\tau} \quad (14)$$

where τ is a dimensionless average deposit thickness:

$$\tau = \frac{\sigma_b i_{avg}}{a\sigma_a zF\rho} = \frac{b_{avg}\sigma_b}{a\sigma_a} \quad (15)$$

The distribution of the deposit thickness is determined by integrating the current distribution over the time steps $d\tau$:

$$B = \frac{b(x,t)\sigma_b}{a\sigma_a} = \int_0^{\tau} I\,d\tau \quad (16)$$

The calculated evolution of the current distribution with the average deposit thickness is shown in Fig. 5. As expected, the nonuniformity decreases as the deposit grows, that is, as the contribution of the deposit to the overall cathode conductance increases. The terminal effect is most pronounced in the early stages of deposition, for $b_{avg} < 5\,\mu m$. Beyond $5\,\mu m$, the current distribution can be considered practically uniform.

Figure 6 shows both calculated and experimental thickness profiles on the resistive plates. The agreement is excellent at $b_{avg} = 2\,\mu m$. At $b_{avg} = 5\,\mu m$ and $10\,\mu m$, however, the experimental profiles are slightly less uniform than the theoretical predictions.

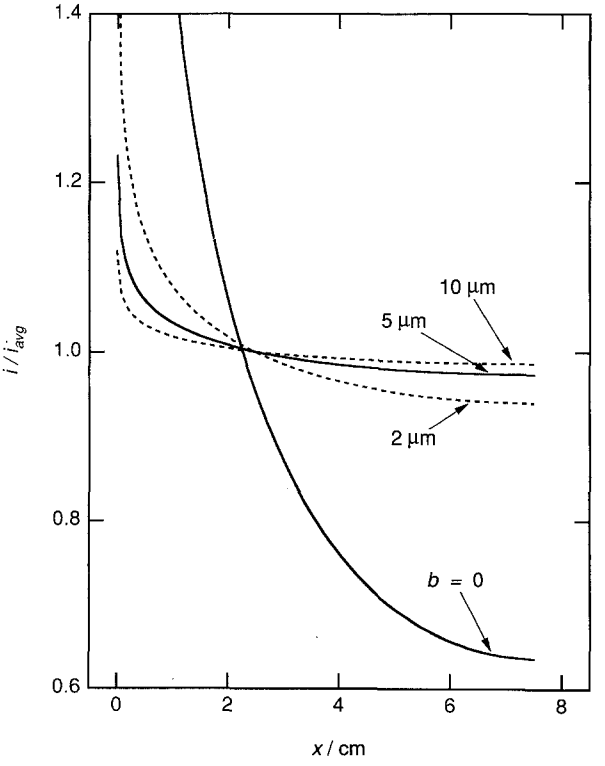

Fig. 5. Change in the calculated primary current distribution with increasing average deposit thickness.

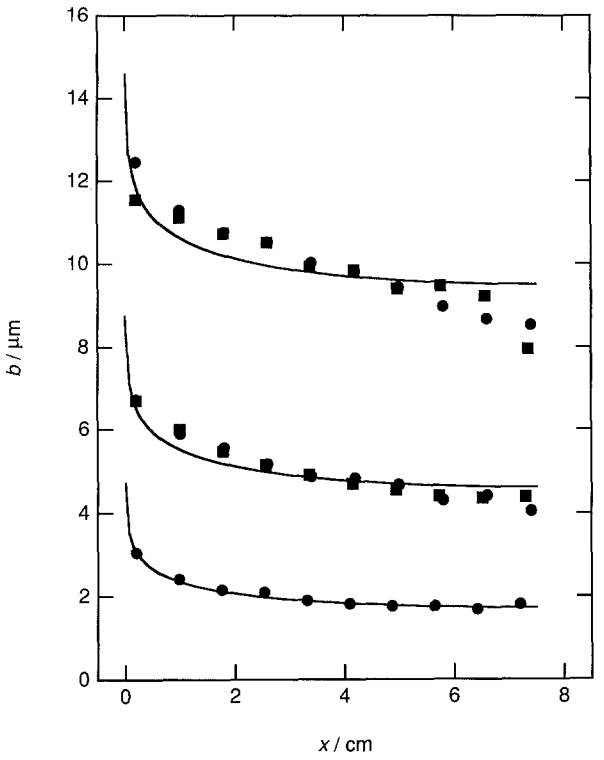

Fig. 6. Experimental thickness profiles of lead deposits on the resistive cathodes and corresponding calculated curves. (●) 60 mA cm^{-2}; (■) 20 mA cm^{-2}; (—) calculation.

Experimental points near the insulated end ($x > 4$ cm) do not follow completely the predicted flat behaviour. This is probably due to the same mass transfer effect observed for the deposits on the nonresistive cathodes (Fig. 4). Thickness measurements on the resistive cathodes do not show this effect immediately, since the current density at the lower end of the cell is initially rather low. As the deposit thickens, however, the current distribution becomes more uniform (Fig. 5) and the current density rises near the insulating end, leading to the same limitations observed for the nonresistive plates. In the worst cases (60 mA cm^{-2}) the drop in deposit thickness due to nonuniform stirring can be as high as 10%. Nevertheless, since a more thorough investigation of the variation of the diffusion-layer thickness with position would be beyond the scope of this work, no account has been taken of the effect in the calculation of the theoretical curves.

5. Conclusions

The present experimental study of lead electrodeposition onto a resistive substrate shows an increase in local deposit thickness near the current collector as predicted by theoretical considerations. Reasonable agreement is found between the experimental results and theoretical predictions taking into account the decrease of the ohmic resistance with increasing deposit thickness.

Acknowledgements

Financial support for this investigation was provided by the Fondation Suisse pour la Recherche en Microtechnique (FSRM) and by the Fonds National Suisse de la Recherche Scientifique, Bern, Switzerland. The authors wish to express their thanks to Helmut Fischer AG, Switzerland for use of their X-ray fluorescence equipment.

References

[1] M. Matlosz, P.-H. Vallotton, A. C. West and D. Landolt, *J. Electrochem. Soc.* **139** (1992) 753.
[2] V. G. Fomichev, *Soviet Electrochemistry* **4** (1968) 708.
[3] J. Wojtowicz, L. Laliberté and B. E. Conway, *Electrochim. Acta* **13** (1968) 361.
[4] J. F. D'Amico, M. A. De Angelo and F. R. McLarnon, *J. Electrochem. Soc.* **132** (1985) 2330.
[5] C. W. Tobias and R. Wijsman, *J. Electrochem. Soc.* **100** (1953) 459.
[6] J. M. Bisang and G. Kreysa, *J. Appl. Electrochem.* **18** (1988) 422.
[7] J. M. Bisang, *ibid.* **19** (1989) 500.
[8] A. Ruffoni and D. Landolt, *Electrochimica Acta* **33** (1988) 1273.
[9] A. Brenner, 'Electrodeposition of Alloys', Vol. 2, Academic Press, New York, chapter 22, pp. 5–16.
[10] T. Cheng and H. Y. Cheh, Abstract 248, The Electrochemical Society Extended Abstracts, Vol. 83–2, Washington DC, 9–14 Oct. (1983) p. 390.
[11] D. T. Chin, *J. Electrochem. Soc.* **118** (1971) 1434.
[12] K. Madry, *Oberfläche – Surface* **27** (1986) 9.
[13] P.-H. Vallotton, Thesis Number 847, Swiss Federal Institute of Technology, Lausanne, Switzerland (1990).